Journal of Engineering Mathematics, Vol. 12, No. 3, July 1978
Sijthoff & Noordhoff International Publishers–Alphen aan den Rijn
Printed in The Netherlands

On compressible flow in a rotating cylinder

J. J. H. BROUWERS

Ultra Centrifuge Nederland N.V., UC-Laboratorium, Almelo, The Netherlands

(Received January 26, 1978)

SUMMARY

Axisymmetric steady flow of a perfect gas in a rotating cylinder is studied by applying a linearised analysis to a small perturbation about isothermal rigid body rotation. Motivated by present day gas centrifuges, special attention is focussed on the effect of a length-to-radius ratio which increases from unit magnitude to infinity and on the effect of a strong radial density gradient associated with the isothermal rigid body rotation. The Ekman number E_* based on the small radial density scale and the density at the cylinder wall is taken to be small. It appears that the flow outside Ekman boundary layers at the end caps consists of three types. These correspond to $1 \ll L_* \ll E_*^{-\frac{1}{2}}$, $E_*^{-\frac{1}{2}} \sim L_* \ll E_*^{-1}$ and $E_*^{-1} \sim L_*$, where L_* is the ratio of the cylinder-length to the radial density scale. For $1 \ll L_* \ll E_*^{-\frac{1}{2}}$ an inviscid flow in a region of limited thickness near the cylinder wall is found. Due to the strong decrease of the density, radial diffusion is not confined to Stewartson boundary layers at the wall (typical for incompressible flow) but extends in the core. This finds expression in two layers in the centre of the cylinder, parallel to the rotation axis, having a structure similar to both Stewartson layers and adjusting the inviscid flow near the wall to a flow dominated by radial diffusion near the rotation axis. For $L_* \sim E_*^{-\frac{1}{2}}$ and $L_* \sim E_*^{-1}$ both Stewartson layers become successively of the same thickness as the density scale. At the same time the corresponding layers in the core go to the wall and join. As a result, for $L_* \geq E_*^{-1}$ radial diffusive processes are significant in the entire cylinder, a situation also known from studies of flows in semi-infinite gas centrifuges.

1. Introduction

Linearised analysis of the almost isothermal rigid body rotation of a perfect gas in a cylinder has revealed two kinds of solution. The first kind [1, 2, 3, 4] is analogous to the type of solutions obtained for incompressible fluids [5] and is characterised by Ekman layers near the end caps and Stewartson layers near the cylinder wall. In the second kind, arising from the study of a cylinder of semi-infinite length [6, 7, 8, 9], radial diffusion of heat and momentum is not confined to Stewartson layers but extends over the entire cross section of the cylinder. These solutions show a decaying behaviour in the direction of the cylinder axis.

In this paper the almost isothermal rigid body rotation of a perfect gas in a cylinder is studied in detail, with special reference to present day gas centrifuges used for uranium enrichment. Emphasis is given to the effect of the length-to-radius ratio and to the effect of the radial density gradient associated with the basic isothermal rigid body rotation. It appears that the solutions mentioned above form special cases in a much more general family of solutions with the Ekman number, the length-to-radius ratio and the ratio of the circumferential speed to the most probable molecular speed of the gas as parameters.

2. The statement of the problem

Consider a cylinder of radius a and length l filled with a viscous, thermally conductive, perfect gas. In rigid rotation at constant angular speed Ω and constant temperature T_0 the density ρ_e is, as a function of the dimensionless radial distance from the rotation axis r, given by

$$\rho_e = \rho_w \exp\{A(r^2 - 1)\}, \tag{2.1}$$

where ρ_w is the density at the cylinder wall, $r = 1$. The speed parameter A is defined as the square of the ratio of the circumferential speed to the most probable molecular speed: i.e.

$$A = \tfrac{1}{2}\Omega^2 a^2 M/R_0 T_0, \tag{2.2}$$

where R_0 is the universal gas constant and M the molecular weight of the gas. From the perfect gas equation one finds for the pressure

$$P_e = \rho_e R_0 T_0/M. \tag{2.3}$$

We consider a small perturbation of this isothermal rigid body rotation, caused by temperature disturbances on the co-rotating horizontal end caps at $z = 0$ and $z = 1$ of the form

$$T_0\{1 + \varepsilon F_1(r)\} \text{ and } T_0\{1 + \varepsilon F_2(r)\},$$

respectively, where z is the dimensionless axial distance and where ε is a small quantity. In the perturbed state we describe temperature, pressure and density with

$$T = T_0(1 + \varepsilon\theta), \tag{2.4}$$

$$P = P_e(1 + \varepsilon p), \tag{2.5}$$

$$\rho = \rho_e(1 + \varepsilon\tau). \tag{2.6}$$

For axisymmetric steady flow the velocity components u, w, v in radial, axial and azimuthal directions respectively, can be expressed in terms of the stream function ψ and the angular speed perturbation ω by

$$u = -\varepsilon\frac{\Omega a^2 r}{\rho l}\frac{\partial}{\partial z}(\rho\psi), \quad w = \varepsilon\frac{\Omega a}{\rho r}\frac{\partial}{\partial r}(\rho r^2\psi), \tag{2.7}$$

$$v = ar\Omega(1 + \varepsilon\omega). \tag{2.8}$$

Upon the neglect of terms of second and higher order in ε the Navier–Stokes equations reduce to

$$\frac{\partial}{\partial z}(2\omega - \theta) = LE\left[\left\{\frac{1}{r}\frac{\partial}{\partial r}\frac{1}{r}e^{-A(r^2-1)}\frac{\partial}{\partial r}r^2 + L^{-2}e^{-A(r^2-1)}\frac{\partial^2}{\partial z^2}\right\}^2\right.$$

$$-\frac{4}{3}\left\{2AL^{-1}e^{-A(r^2-1)}r\frac{\partial}{\partial z}\right\}^2\Bigg]e^{A(r^2-1)}\psi, \tag{2.9}$$

$$-2\frac{\partial\psi}{\partial z} = LEe^{-A(r^2-1)}\left\{\frac{1}{r}\frac{\partial}{\partial r}\frac{1}{r}\frac{\partial}{\partial r}r^2 + L^{-2}\frac{\partial^2}{\partial z^2}\right\}\omega, \tag{2.10}$$

where L is the aspect ratio,

$$L = l/a, \tag{2.11}$$

and E the Ekman number based on the radius of the cylinder and based on the density at the cylinder wall,

$$E = \mu/\rho_w\Omega a^2, \tag{2.12}$$

μ being the dynamic viscosity. Equation (2.9) results from elimination of p between the radial and axial momentum equations, (2.10) is the azimuthal momentum equation. The terms on the right hand sides of (2.9) and (2.10) represent viscous forces, which are balanced by Coriolis forces, centrifugal forces and pressure gradients. The energy equation is, in linearised form

$$r^2 Br\frac{\partial\psi}{\partial z} = LEe^{-A(r^2-1)}\left\{\frac{1}{r}\frac{\partial}{\partial r}r\frac{\partial}{\partial r} + L^{-2}\frac{\partial^2}{\partial z^2}\right\}\theta, \tag{2.13}$$

where Br is the Brinkman number [10]

$$Br = \mu\Omega^2 a^2/\kappa T_0, \tag{2.14}$$

κ being the thermal conductivity. The term on the left hand side of (2.13) represents the work done by compression when the fluid moves radially $(u(\partial/\partial r)P)$, which is balanced by heat conduction. The boundary conditions are such that the velocities and temperatures coincide with those of the walls: i.e.

$$\omega = \psi = (\partial/\partial r)\psi = \theta = 0 \qquad \text{at } r = 1, \tag{2.15a}$$

$$\omega = \psi = (\partial/\partial z)\psi = 0 \qquad \text{at } z = 0 \text{ and } z = 1, \tag{2.15b}$$

$$\theta = F_1(r), \quad r < 1, \qquad \text{at } z = 0, \tag{2.15c}$$

$$\theta = F_2(r), \quad r < 1, \qquad \text{at } z = 1, \tag{2.15d}$$

where F_1 and F_2 are smooth functions of r.

The Ekman number is taken to be small and the Brinkman number is of unit magnitude. The case that the speed parameter is of unit magnitude and the case that the speed parameter is large will be discussed. The aspect ratio is varied from unit magnitude to infinity.

The dynamical equations (2.9), (2.10) and (2.13) are transformed into

$$2\frac{\partial\chi}{\partial z} = LE\left[\left\{\frac{1}{r}\frac{\partial}{\partial r}\frac{1}{r}e^{-A(r^2-1)}\frac{\partial}{\partial r}r^2 + L^{-2}e^{-A(r^2-1)}\frac{\partial^2}{\partial z^2}\right\}^2 - \frac{4}{3}\left\{2AL^{-1}e^{-A(r^2-1)}r\frac{\partial}{\partial z}\right\}^2\right]e^{A(r^2-1)}\psi, \tag{2.16}$$

$$-2(1+\tfrac{1}{4}r^2Br)\frac{\partial\psi}{\partial z} = LEe^{-A(r^2-1)}\left[\left\{\frac{1}{r}\frac{\partial}{\partial r}\frac{1}{r}(1+\tfrac{1}{4}r^2Br)\frac{\partial}{\partial r}(1+\tfrac{1}{4}r^2Br)^{-1}r^2 + L^{-2}\frac{\partial^2}{\partial z^2}\right\}\chi + \frac{1}{r}\frac{\partial}{\partial r}(1+\tfrac{1}{4}r^2Br)^{-1}\phi\right], \tag{2.17}$$

$$\left\{\frac{1}{r}\frac{\partial}{\partial r}r(1+\tfrac{1}{4}r^2Br)\frac{\partial}{\partial r}(1+\tfrac{1}{4}r^2Br)^{-1} + L^{-2}\frac{\partial^2}{\partial z^2}\right\}\phi = Br\frac{1}{r}\frac{\partial}{\partial r}r^2(1+\tfrac{1}{4}r^2Br)^{-1}\chi, \tag{2.18}$$

where

$$\chi = \omega - \tfrac{1}{2}\theta,\ \phi = \theta + \tfrac{1}{2}r^2Br\omega. \tag{2.19}$$

Here, equation (2.16) is the same as (2.9). Equation (2.17) is obtained by multiplying (2.13) with $\frac{1}{2}$ and subtracting this from (2.10). Equation (2.18) is found by eliminating $(\partial/\partial z)\psi$ from (2.10) and (2.13). The equation for ϕ, (2.18), is only coupled to those for χ and ψ, (2.16) and (2.17), by means of the term in ϕ on the right hand side of (2.17). Consider the meaning of this term for the cases of interest. In case of an inviscid flow for ψ and χ, extended by boundary layers, the term in ϕ is insignificant. In an inviscid domain the entire right hand side of (2.17) can be neglected. In thin boundary layers the term is still negligible since it does not contain the highest derivatives with respect to r and z. On the other hand, the term in ϕ becomes significant when radial diffusion of χ is important in a region of radial extent comparable with the radius. For $A \sim 1$ this happens when L is large (since L multiplies the small E in (2.17)) and, as a result, the z-derivatives of ϕ in (2.18) can be neglected.

Integrating the remaining equation with respect to r and requiring that ϕ and χ are finite as $r \to 0$, one gets

$$\frac{1}{r}\frac{\partial}{\partial r}(1+\tfrac{1}{4}r^2Br)^{-1}\phi = Br(1+\tfrac{1}{4}r^2Br)^{-2}\chi, \tag{2.20}$$

a result that can be used to eliminate the term in ϕ on the right of (2.17). For $A \gg 1$ it appears that $\partial/\partial r \sim A$ (see section 4) so that the z-derivatives in (2.18) can be neglected when $L^2A^2 \gg 1$, which applies when L is of unit magnitude or larger. Therefore, in all cases of interest (2.20) may be substituted into (2.17). We are now in the fortunate position that only these two equations have to be considered in order to obtain a solution for χ and ψ. This is especially advantageous for gas centrifuge problems where one is mainly interested in the distribution of the axial and radial velocity. The small perturbations of the angular speed and temperature are of less importance so that the extra equation (2.18) does not need to be considered. Substitution of (2.20) into (2.17) gives for χ and ψ the equations

$$2\frac{\partial\chi}{\partial z} = LE\left[\left\{\frac{1}{r}\frac{\partial}{\partial r}\frac{1}{r}e^{-A(r^2-1)}\frac{\partial}{\partial r}r^2 + L^{-2}e^{-A(r^2-1)}\frac{\partial^2}{\partial z^2}\right\}^2 - \frac{4}{3}\left\{2AL^{-1}e^{-A(r^2-1)}r\frac{\partial}{\partial z}\right\}^2\right]e^{A(r^2-1)}\psi, \tag{2.21}$$

$$-2\frac{\partial\psi}{\partial z} = LE^{-A(r^2-1)}\left[\frac{1}{r^3}\frac{\partial}{\partial r}(1+\tfrac{1}{4}r^2Br)^{-1}r^3\frac{\partial}{\partial r} + (1+\tfrac{1}{4}r^2Br)^{-1}L^{-2}\frac{\partial^2}{\partial z^2}\right]\chi. \tag{2.22}$$

The boundary conditions are

$$\chi = \psi = (\partial/\partial r)\psi = 0 \qquad \text{at } r = 1, \tag{2.23a}$$

$$\psi = (\partial/\partial z)\psi = 0 \qquad \text{at } z = 0 \text{ and } z = 1, \tag{2.23b}$$

$$\chi = -\tfrac{1}{2}F_1(r), \quad r < 1, \qquad \text{at } z = 0, \tag{2.23c}$$

$$\chi = -\tfrac{1}{2}F_2(r), \quad r < 1, \qquad \text{at } z = 1, \tag{2.23d}$$

where F_1 and F_2 are smooth functions of r.

3. The small density gradient

Consider the case $A \sim 1$. Replacing χ by ω one sees that the differential equations (2.21) and (2.22) with boundary conditions (2.23) are quite similar to those given by Greenspan [5] and Stewartson [11] for an incompressible fluid. The exponential function stemming from the density distribution at isothermal rigid body rotation is of unit magnitude and does not change the magnitude of the terms in which it occurs. The same applies to the terms formed with the Brinkman number since $Br \sim 1$. A similar procedure as usually applied to incompressible cases is therefore appropriate. In the limit of $E \to 0$ equations (2.21) and (2.22) reduce to

$$(\partial/\partial z)\chi = 0, \quad (\partial/\partial z)\psi = 0, \tag{3.1}$$

which implies that the axial velocity and a combination of the angular speed and temperature given by $\omega - \frac{1}{2}\theta$ are constant with respect to z, a result that may be referred to as the compressible Taylor–Proudman theorem. Ekman layers of thickness $L^{-1}E^{\frac{1}{2}}$ adjust the inviscid flow to the end caps. An outer Stewartson layer of thickness $L^{\frac{1}{4}}E^{\frac{1}{4}}$ and an inner Stewartson layer of thickness $L^{\frac{1}{3}}E^{\frac{1}{3}}$ bring the inviscid variables to zero at the cylinder wall. This flow type is well known from the literature [1, 2, 3, 4] and follows from a modification of the incompressible case. The boundary layer thicknesses are small if $E^{\frac{1}{2}} \ll L \ll E^{-\frac{1}{3}}$, which covers most configurations. When, however, the aspect ratio exceeds the upper limit of this range, both Stewartson layers successively fill the entire cylinder and radial diffusive processes become important when describing the flow field in the main section.

The flow discussed above is only applicable when the speed parameter is of unit magnitude. In gas centrifuges A is quite large and then the solution of (2.21) and (2.22) is quite different from incompressible flow.

4. The large density gradient

The working fluid in a centrifuge is gaseous uranium hexafluoride (UF_6). The most probable molecular speed $\sqrt{2R_0T_0/M}$ of UF_6 is approximately 120 m/s at room temperature. This quantity is relatively small due to the large molecular weight of UF_6 (air: $\sqrt{2R_0T_0/M} \approx 480$ m/s). Circumferential speeds of 500 m/s or more are quite normal today. Taking $\Omega a = 500$ m/s the speed parameter A becomes: $A \approx 17$. Consider the consequences of such a large A. Inspection of (2.21) and (2.22) shows that the density function $\exp\{A(r^2-1)\}$ forms, with the Ekman number, a local Ekman number $E\exp\{A(1-r^2)\}$. Although this local Ekman number is small at $r = 1$ it increases very rapidly with distance from the cylinder wall: e.g. for $A = 17$, $\exp\{A(1-r^2)\} \approx 25$ at $r = 0.9$ and 2.4×10^7 at $r = 0$. Furthermore, the presence of the density function makes that all variables depend on $\exp\{A(1-r^2)\}$: derivatives with respect to r will not be of unit magnitude but $(\partial/\partial r) \sim A$. In order to perform an adequate scaling analysis it is convenient to introduce a coordinate, measured from the cylinder wall, which corresponds to a change of unit magnitude of the density function: i.e.

$$x = A(1-r^2), \quad 0 \le x \le A. \tag{4.1}$$

Furthermore we introduce

$$\psi^* = A\psi. \tag{4.2}$$

Dropping the asterisk on ψ equations (2.21) and (2.22) become

$$2\frac{\partial \chi}{\partial z} = L_* E_* \left[\left\{4\frac{\partial}{\partial x} e^x \frac{\partial}{\partial x}\left(1-\frac{x}{A}\right) + L_*^{-2} e^x \frac{\partial^2}{\partial z^2}\right\}^2 - \frac{4}{3}\left(1-\frac{x}{A}\right)\left\{2L_*^{-1} e^x \frac{\partial}{\partial z}\right\}^2\right] e^{-x}\psi, \tag{4.3}$$

$$-2\frac{\partial \psi}{\partial z} = L_* E_* e^x \left[4\left(1-\frac{x}{A}\right)^{-1} \frac{\partial}{\partial x}\left\{1+\tfrac{1}{4}Br\left(1-\frac{x}{A}\right)\right\}^{-1}\left(1-\frac{x}{A}\right)^2 \frac{\partial}{\partial x} + \left\{1+\tfrac{1}{4}Br\left(1-\frac{x}{A}\right)\right\}^{-1} L_*^{-2}\frac{\partial^2}{\partial z^2}\right]\chi. \tag{4.4}$$

The boundary conditions are

$$\chi = \psi = (\partial/\partial x)\psi = 0 \qquad \text{at } x = 0, \tag{4.5a}$$

$$\psi = (\partial/\partial z)\psi = 0 \qquad \text{at } z = 0 \text{ and } z = 1, \tag{4.5b}$$

$$\chi = -\tfrac{1}{2}F_1(x), \quad x > 0 \qquad \text{at } z = 0, \tag{4.5c}$$

$$\chi = -\tfrac{1}{2}F_2(x), \quad x > 0 \qquad \text{at } z = 1, \tag{4.5d}$$

where F_1 and F_2 are smooth functions of x. The modified Ekman number E_* and the modified aspect ratio L_* are based on the scale of the density decrease instead of the radius. These are related to E and L by

$$E_* = EA^2, \quad L_* = LA. \tag{4.6}$$

Returning to the size and operational conditions of a gas centrifuge we take for the radius 10^{-1} m and 8000 N/m^2 for the UF_6 pressure at the cylinder wall. The viscosity of UF_6 is 1.69×10^{-5} kg/ms, the heat conductivity is 6.68×10^{-3} W/mK. These values correspond to $E_* \approx 10^{-4}$ and $Br \approx 2$. Therefore we consider in the following $A \gg 1$, $E_* \ll 1$ and $Br \sim 1$. Gas centrifuges have an aspect ratio which is of unit magnitude or larger. Since $L_* = LA$ we take $L_* \gg 1$.

In the limit of $E_* \to 0$ we obtain (3.1) by which we are unable to satisfy the boundary conditions for χ and ψ. Just as with incompressible flow Ekman layers have to be introduced at the end caps and Stewartson layers at the cylinder wall. In the compressible case there are complications however. Putting, led by experience in incompressible flow, in the interior

$$\chi = \chi_0, \quad \psi = (E_* e^x)^{\frac{1}{2}} \psi_0, \tag{4.7}$$

and introducing this into (4.3) and (4.4), it follows that the terms on the right hand side have orders $L_*(E_*e^x)^{\frac{1}{2}}$, $L_*^{-1}(E_*e^x)^{\frac{1}{2}}$, $L_*^{-3}(E_*e^x)^{\frac{1}{2}}$, $L_*(E_*e^x)^{\frac{1}{2}}$ and $L_*^{-1}(E_*e^x)^{\frac{1}{2}}$ compared to those on the left hand sides. All these terms are small if

$$(E_*e^x)^{\frac{1}{2}} \ll L_* \ll (E_*e^x)^{-\frac{1}{2}}, \tag{4.8}$$

where E_* is supposed to be small, but where e^x increases from 1 to e^A which is supposed to be very large.

An inviscid flow can be expected if $E_*^{\frac{1}{2}} \ll L_* \ll E_*^{-\frac{1}{2}}$, but, due to the increase of e^x with distance from the cylinder wall, such an inviscid flow is only observed in a limited region near the cylinder wall. Consider for example the case $L_* \sim 1$. Then condition (4.8) is only satisfied for $x \ll \ln E_*^{-1}$ (for $E_* = 10^{-4}$ this means $x \ll 10$). At $x \sim \ln E_*^{-1}$ the local modified Ekman number, E_*e^x, is of unit magnitude and here áll terms on the right hand sides of (4.3) and (4.4) are comparable to those on the left. Of course since x is at most A (the rotation axis), such an "all terms diffusive core" does not occur when $\ln E_*^{-1} \gg A$.

We are concerned with the case $L_* \gg 1$. Then we can conclude from (4.8) that an inviscid flow is only observed if

$$1 \ll L_* \ll E_*^{-\frac{1}{2}}, \tag{4.9a}$$

in a region near the cylinder wall given by

$$x \ll \ln (L_*^2 E_*)^{-1}. \tag{4.9b}$$

In the following we refer to the range (4.9a) as THE UNIT CYLINDER. The diffusive flow at $x \geq \ln (L_*^2 E_*)^{-1}$ will be investigated in greater detail in Section 5 below.

The inviscid solution cannot satisfy the boundary conditions at the end caps. To overcome this non-uniformity layers of the Ekman type are needed. For these layers we introduce

$$\chi = \tilde{\chi}_0,\ \psi = (E_* e^x)^{\frac{1}{2}} \tilde{\psi}_0,\ \tfrac{1}{2} - \tfrac{1}{2} j - z = -j L_*^{-1} (E_* e^x)^{\frac{1}{2}} y, \tag{4.10}$$

where $j = +1$ at the bottom and $j = -1$ at the top. In terms of these variables and letting $(E_* e^x)^{\frac{1}{2}} \to 0$ the equations (4.3) and (4.4) become

$$2j \frac{\partial \tilde{\chi}_0}{\partial y} = \frac{\partial^4 \tilde{\psi}_0}{\partial y^4}, \tag{4.11}$$

$$-2j \left\{1 + \tfrac{1}{4} Br\left(1 - \frac{x}{A}\right)\right\} \frac{\partial \tilde{\psi}_0}{\partial y} = \frac{\partial \tilde{\chi}_0^2}{\partial y^2}. \tag{4.12}$$

Just as in incompressible flow the thickness of the Ekman layer is proportional to the square root of the kinematic viscosity $\nu = \mu/\rho$. But in the compressible case the density decreases with distance from the cylinder wall and therefore the layer becomes thicker with increasing x (see (4.10)).

Furthermore, in deriving (4.11) and (4.12) terms $\sim (E_* e^x)^{\frac{1}{2}}$ have been neglected. This is no longer justified at $x \sim \ln E_*^{-1}$ where all terms of the original equations become important and where the layer has increased to a thickness $\sim L_*^{-1}$. This shows that the approximation of inviscid flow and Ekman layers is not uniformly valid up to the rotation axis. As long as $x \ll \ln E_*^{-1}$ (4.11) and (4.12) describe a boundary layer flow within which only axial diffusion is significant. From equations (4.11) and (4.12) with boundary conditions (4.5b), (4.5c) and (4.5d) the Ekman suction conditions for the flow outside the boundary layers are obtained as*

$$\left\{1 + \tfrac{1}{4} Br\left(1 - \frac{x}{A}\right)\right\}^{\frac{3}{4}} \psi - \tfrac{1}{2}(E_* e^x)^{\frac{1}{2}} \chi = +\tfrac{1}{4}(E_* e^x)^{\frac{1}{2}} F_1 \ \text{ at } z = 0, \tag{4.13a}$$

$$\left\{1 + \tfrac{1}{4} Br\left(1 - \frac{x}{A}\right)\right\}^{\frac{3}{4}} \psi + \tfrac{1}{2}(E_* e^x)^{\frac{1}{2}} \chi = -\tfrac{1}{4}(E_* e^x)^{\frac{1}{2}} F_2 \ \text{ at } z = 1, \tag{4.13b}$$

provided that

$$0 < x \ll \ln E_*^{-1}. \tag{4.13c}$$

Applying these conditions on the inviscid flow one finds

$$\chi_0 = -\tfrac{1}{4}\{F_1 + F_2\},\ \psi_0 = \frac{1}{8}\left\{1 + \tfrac{1}{4} Br\left(1 - \frac{x}{A}\right)\right\}^{-\frac{3}{4}} \{F_1 - F_2\}, \tag{4.14a}$$

provided that (cf. (4.9b))

* Differential rotation of the end caps or axial injection and removal of fluid at the end caps can be fitted in the functions F_1 and F_2 in (4.13): the presented solutions for the flow outside the Ekman layers remain qualitatively unaffected [12].

$$0 < x \ll \ln (L_*^2 E_*)^{-1}, \tag{4.14b}$$

where χ_0 and ψ_0 are defined by (4.7).

For $F_1(0+) \neq 0$ and $F_2(0+) \neq 0$ solution (4.14) does not satisfy the boundary conditions at the cylinder wall. Therefore two layers of the type first discussed by Stewartson [11] are needed. The scaling rules for the inner layer are

$$\chi = L_*^{-\frac{1}{3}} E_*^{\frac{1}{6}} \tilde{\chi}_1, \; \psi = E_*^{\frac{1}{2}} \tilde{\psi}_1, \; x = (L_* E_*)^{\frac{1}{3}} \zeta_1. \tag{4.15}$$

Putting (4.15) into (4.3) and (4.4), and letting $L_*^{-1} E_*^{\frac{1}{2}} \to 0$ and $L_* E_* \to 0$, the equations become

$$\frac{\partial \tilde{\chi}_1}{\partial z} = 8 \frac{\partial^4 \tilde{\psi}_1}{\partial \zeta_1^4}, \tag{4.16}$$

$$-(1 + \tfrac{1}{4} Br) \frac{\partial \tilde{\psi}_1}{\partial z} = 2 \frac{\partial^2 \tilde{\chi}_1}{\partial \zeta_1^2}. \tag{4.17}$$

The scaling rules for the outer layer are

$$\chi = \tilde{\chi}_2, \; \psi = E_*^{\frac{1}{2}} \tilde{\psi}_2, \; x = L_*^{\frac{1}{2}} E_*^{\frac{1}{4}} \zeta_2. \tag{4.18}$$

Substituting (4.18) into (4.3) and (4.4), and letting $L_*^{-1} E_*^{\frac{1}{2}} \to 0$ and $L_* E_*^{\frac{1}{2}} \to 0$, we obtain

$$\frac{\partial \tilde{\chi}_2}{\partial z} = 0, \; -(1 + \tfrac{1}{4} Br) \frac{\partial \tilde{\psi}_2}{\partial z} = 2 \frac{\partial^2 \tilde{\chi}_2}{\partial \zeta_2^2}. \tag{4.19}$$

Both layers are terminated at top and bottom by Ekman layers. The outer layer adjusts χ, but not in its second derivative with respect to x, and the inner one completes the adjustment and brings ψ to zero at $x = 0$ [13]. Equations (4.16), (4.17) and (4.19) with appropriate boundary conditions do not essentially differ from those given for incompressible flow. This is due to the requirements $L_* \ll E_*^{-\frac{1}{2}}$ and $L_* \ll E_*^{-1}$ for outer and inner layer respectively, by which the density is constant over the layers ($e^x = 1$). When $L_* \geq E_*^{-\frac{1}{2}}$ the thicknesses of both layers become successively comparable with the distance over which the density decreases appreciably. According to (4.9), however, diffusion comes up from the core in that case and an inviscid flow no longer exists. When Stewartson layers occur they are regions of virtually constant density.

5. The diffusive core

The approximation of inviscid flow is not uniformly valid up to the rotation axis. Physically this can be understood by noting that at constant dynamic viscosity the kinematic viscosity varies as ρ^{-1}. Since the density decreases strongly with the distance from the cylinder wall, the flow becomes more and more viscous. For an analysis of the viscous flow in the core we consider THE UNIT CYLINDER: $1 \ll L_* \ll E_*^{-\frac{1}{2}}$. Since L_*^{-1} is small the z-derivatives on the right hand side of (4.3) and (4.4) can be neglected compared to the x-derivatives, independent on the magnitude of e^x, with the result that

$$\frac{\partial \chi}{\partial z} = 8L_* E_* \left\{ \frac{\partial}{\partial x} e^x \frac{\partial}{\partial x}\left(1 - \frac{x}{A}\right)\right\}^2 e^{-x}\psi \tag{5.1}$$

and

$$-\frac{\partial \psi}{\partial z} = 2L_* E_* e^x \left(1 - \frac{x}{A}\right)^{-1} \frac{\partial}{\partial x}\left\{1 + \tfrac{1}{4}Br\left(1 - \frac{x}{A}\right)\right\}^{-1}\left(1 - \frac{x}{A}\right)^2 \frac{\partial \chi}{\partial x}. \tag{5.2}$$

The boundary conditions at $z = 0$ and $z = 1$ are given by the Ekman suction conditions, (4.13). These conditions are only applicable as long as $x \ll \ln E_*^{-1}$ but, as will be shown in the subsequent analysis, this forms no limitation for the description of the main flow field in the core. Introducing

$$x = \eta_1 + \ln(L_* E_*)^{-1}, \ \chi = bL_*^{-\frac{1}{2}}\bar{\chi}_1, \ \psi = bL_*^{-\frac{1}{2}}\bar{\psi}_1, \tag{5.3}$$

where b is (at present) an arbitrary constant, equations (5.1) and (5.2) become to lowest order

$$\frac{\partial \bar{\chi}_1}{\partial z} = 8\alpha_1^2 \left\{ \frac{\partial}{\partial \eta_1} e^{\eta_1} \frac{\partial}{\partial \eta_1}\right\}^2 e^{-\eta_1}\bar{\psi}_1, \tag{5.4}$$

$$-(1 + \tfrac{1}{4}\alpha_1 Br)\frac{\partial \bar{\psi}_1}{\partial z} = 2\alpha_1 e^{\eta_1}\frac{\partial^2 \bar{\chi}_1}{\partial \eta_1^2}, \tag{5.5}$$

where

$$\alpha_1 = 1 - A^{-1}\ln(L_* E_*)^{-1}. \tag{5.6}$$

In the following we refer to the above deduced viscous layer at $x \sim \ln(L_* E_*)^{-1}$ as the *inner layer*. In terms of the radial coordinate its position is given by $r^2 \sim \alpha_1$. In deriving (5.4) and (5.5) we approximated $1 - x/A$ by the constant α_1: i.e.

$$1 - x/A = \alpha_1 - A^{-1}\eta_1 \sim \alpha_1. \tag{5.7}$$

This is valid as long as

$$\alpha_1 A \gg 1, \tag{5.8}$$

which implies that the inner layer must be situated at a radial position that is large compared to $A^{-\frac{1}{2}}$ or $r^2 \gg A^{-1}$. When it is situated somewhere in the middle of the cylinder (α_1 of unit magnitude) condition (5.8) is satisfied since we took $A \gg 1$. The exponential increase of the terms on the right of (5.1) and (5.2) is responsible for the above balance at $x \sim \ln(L_* E_*)^{-1}$. Similarly, for $x \gg \ln(L_* E_*)^{-1}$ the diffusive terms dominate over the inertia terms, whence

$$\left\{\frac{1}{r}\frac{\partial}{\partial r}\frac{1}{r}e^{-A(r^2-1)}\frac{\partial}{\partial r}r^2\right\}^2 e^{A(r^2-1)}\psi_d = 0, \tag{5.9}$$

$$\frac{1}{r^3}\frac{\partial}{\partial r}(1+\tfrac{1}{4}r^2Br)^{-1}r^3\frac{\partial\chi_d}{\partial r}=0, \tag{5.10}$$

where we reintroduced the coordinate r. Integrating (5.9) and (5.10) with respect to r and requiring that the angular velocity, temperature and axial velocity are finite as $r\to 0$ and that the radial mass flow is zero at $r=0$, one gets

$$\psi_d = C_1(1-e^{-Ar^2})/r^2,\ \chi_d = C_2. \tag{5.11}$$

These "pure diffusive solutions" describe the flow between the inner layer and the rotation axis. The integration constants C_1 and C_2 are found by matching (5.11) to the inner layer solution. Expanding r^2 in (5.11) in terms of the coordinate η_1 it follows that χ_d and ψ_d are constant with respect to η_1, provided that (5.8) is satisfied. The boundary conditions for the inner layer are therefore

$$(\partial/\partial\eta_1)\bar{\chi}_1 \sim 0,\ (\partial/\partial\eta_1)\bar{\psi}_1 \sim 0 \ \text{ as } \eta_1\to\infty. \tag{5.12}$$

Putting (5.3) into (4.13) and dropping terms $\sim L_*^{-\frac{1}{2}}$ and $\sim\alpha_1^{-1}A^{-1}$ compared to unit magnitude, the Ekman suction conditions for the inner layer become

$$\bar{\psi}_1 = +\tfrac{1}{4}\{1+\tfrac{1}{4}Br\alpha_1\}^{-\frac{3}{4}}b^{-1}e^{\frac{1}{2}\eta_1}F_1 \qquad \text{at } z=0, \tag{5.13}$$

$$\bar{\psi}_1 = -\tfrac{1}{4}\{1+\tfrac{1}{4}Br\alpha_1\}^{-\frac{3}{4}}b^{-1}e^{\frac{1}{2}\eta_1}F_2 \qquad \text{at } z=1. \tag{5.14}$$

For $\eta_1\to-\infty$ the inner layer must match the inviscid solution. In the inviscid region $\chi\sim F_1, F_2$ and $\psi\sim E_*^{\frac{1}{2}}e^{\frac{1}{2}x}F_1$ $(=L_*^{-\frac{1}{2}}e^{\frac{1}{2}\eta_1}F_1)$, $E_*^{\frac{1}{2}}e^{\frac{1}{2}x}F_2$ $(=L_*^{-\frac{1}{2}}e^{\frac{1}{2}\eta_1}F_2)$. Consider the case that the inner layer adjusts χ. Then we must take $b=L_*^{\frac{1}{2}}$ in (5.3), if $F_1\sim 1$ and $F_2\sim 1$ at $\eta_1\sim 1$, and since $L_*\gg 1$ (5.13) and (5.14) reduce to

$$\bar{\psi}_1 = 0 \qquad \text{at } z=0 \text{ and } z=1. \tag{5.15}$$

Integrating (5.5) with respect to z from 0 to 1 and applying (5.15) it follows that

$$\frac{\partial^2}{\partial\eta_1^2}\left(\int_0^1\bar{\chi}_1\,dz\right)=0. \tag{5.16}$$

One sees that

$$\int_0^1\bar{\chi}_1\,dz \tag{5.17}$$

is a linear function of η_1 and, consequently, cannot tend to two different finite values as $\eta_1\to\pm\infty$. As a result, the inner layer cannot adjust χ to its pure diffusive value near the rotation axis. Therefore a second layer, referred to in the following as the *outer layer*, is needed. The inner layer is used to adjust ψ which means $b=1$ in (5.3).

Introducing

$$x=\eta_2+\ln(L_*^2E_*)^{-1},\ \chi=\bar{\chi}_2,\ \psi=L_*^{-1}\bar{\psi}_2, \tag{5.18}$$

into (5.1) and (5.2), and letting $L_*^{-2} \to 0$, we obtain

$$\frac{\partial \bar{\chi}_2}{\partial z} = 0, \tag{5.19}$$

$$-\frac{\partial \bar{\psi}_2}{\partial z} = 2e^{\eta_2}\left(\alpha_2 - \frac{\eta_2}{A}\right)^{-1} \frac{\partial}{\partial \eta_2}\left\{1 + \tfrac{1}{4}Br\left(\alpha_2 - \frac{\eta_2}{A}\right)\right\}^{-1}\left(\alpha_2 - \frac{\eta_2}{A}\right)^2 \frac{\partial \bar{\chi}_2}{\partial \eta_2}, \tag{5.20}$$

where

$$\alpha_2 = 1 - A^{-1}\ln(L_*^2 E_*)^{-1}. \tag{5.21}$$

Applying the Ekman suction conditions one finds from (5.19) and (5.20) that

$$\bar{\psi}_2 = \frac{1}{2}\left\{1 + \tfrac{1}{4}Br\left(\alpha_2 - \frac{\eta_2}{A}\right)\right\}^{-\frac{1}{2}} e^{\frac{1}{2}\eta_2}\{\bar{\chi}_2 + \tfrac{1}{2}F_1 - z(\tfrac{1}{2}F_1 + \tfrac{1}{2}F_2 + 2\bar{\chi}_2)\}. \tag{5.22}$$

Putting (5.22) into (5.20) one gets

$$2\left\{1 + \tfrac{1}{4}Br\left(\alpha_2 - \frac{\eta_2}{A}\right)\right\}^{-\frac{1}{2}} e^{\frac{1}{2}\eta_2}\left(\alpha_2 - \frac{\eta_2}{A}\right)^{-1} \frac{d}{d\eta_2} \times$$
$$\times \left\{1 + \tfrac{1}{4}Br\left(\alpha_2 - \frac{\eta_2}{A}\right)\right\}^{-1}\left(\alpha_2 - \frac{\eta_2}{A}\right)^2 \frac{d\bar{\chi}_2}{d\eta_2} - \bar{\chi}_2 = \tfrac{1}{4}(F_1 + F_2). \tag{5.23}$$

In principle, equations (5.22) and (5.23) contain all terms necessary for a description of the flow in the region between the inner layer in the core and the Stewartson layers near the cylinder wall. Consider the inviscid region. For $\eta_2 \sim -\ln(L_*^2 E_*)^{-1}$ the first term on the left of (5.23) becomes small with the result that $\bar{\chi}_2 \sim -\frac{1}{4}(F_1 + F_2)$, which is exactly the inviscid solution. Furthermore, putting this result into (5.22) one obtains the inviscid solution for ψ. However, we are interested in the region $\eta_2 \sim 1$, referred to as the outer layer, where radial diffusion of χ is important. In this region more analytical progress can be made by requiring

$$\alpha_2 A \gg 1, \tag{5.24}$$

which implies that the outer layer must be situated at a radial position that is large compared to $A^{-\frac{1}{2}}$ (note in passing that the outer layer is situated at $r^2 \sim \alpha_2$). In this case the term $\alpha_2 - \eta_2/A$ can be approximated by the constant α_2 by which (5.23) simplifies to

$$2\alpha_2(1 + \tfrac{1}{4}\alpha_2 Br)^{-\frac{1}{2}} e^{\frac{1}{2}\eta_2} \frac{d^2\bar{\chi}_2}{d\eta_2^2} - \bar{\chi}_2 = \tfrac{1}{4}(F_1 + F_2). \tag{5.25}$$

For $\eta_2 \to -\infty$ $\bar{\chi}_2$ must match the inviscid solution: i.e.

$$\bar{\chi}_2 \sim -\tfrac{1}{4}(F_1 + F_2) \quad \text{as } \eta_2 \to -\infty. \tag{5.26}$$

For $\eta_2 \to +\infty$ $\bar{\chi}_2$ must match the inner layer. As was shown above, in the inner layer χ is up to $O(L_*^{-\frac{1}{2}})$ continuous with respect to x and therefore the outer layer directly brings χ to its pure diffusive value: i.e.

$$(d/d\eta_2)\bar{\chi}_2 \sim 0 \quad \text{as } \eta_2 \to +\infty. \tag{5.27}$$

Differential equation (5.25) with boundary conditions (5.26) and (5.27) can be solved by means of the Hankeltransform of zero order [12].

In the region between inner and outer layer, $0 \ll \eta_2 \ll \ln L_*$, the first term on the left of (5.23) dominates over the second one (since $e^{\frac{1}{2}\eta_2}$ is large) with the result that

$$\frac{d}{d\eta_2}\left\{1 + \tfrac{1}{4}Br\left(\alpha_2 - \frac{\eta_2}{A}\right)\right\}^{-1}\left(\alpha_2 - \frac{\eta_2}{A}\right)^2 \frac{d\bar{\chi}_2}{d\eta_2} =$$

$$= \frac{1}{8}\left\{1 + \tfrac{1}{4}Br\left(\alpha_2 - \frac{\eta_2}{A}\right)\right\}^{-\frac{3}{4}}\left(\alpha_2 - \frac{\eta_2}{A}\right)e^{-\frac{1}{2}\eta_2}\{F_1 + F_2\}. \tag{5.28}$$

According to (5.28) $\bar{\chi}_2 \sim e^{-\frac{1}{2}\eta_2}F_1, e^{-\frac{1}{2}\eta_2}F_2$ and since $\eta_2 \gg 0$ (5.22) may be simplified to

$$\bar{\psi}_2 = \frac{1}{4}\left\{1 + \tfrac{1}{4}Br\left(\alpha_2 - \frac{\eta_2}{A}\right)\right\}^{-\frac{3}{4}} e^{\frac{1}{2}\eta_2}\{F_1 - z(F_1 + F_2)\}. \tag{5.29}$$

These solutions describe the flow in the region between inner and outer layer and are used to determine the conditions for the inner layer when $\eta_1 \to \infty$. Expanding the outer layer variables in (5.28) and (5.29) into those of the inner layer and then letting $\alpha_1^{-1}A^{-1} \to 0$, we obtain

$$\bar{\psi}_1 \sim \tfrac{1}{4}(1 + \tfrac{1}{4}\alpha_1 Br)^{-\frac{3}{4}} e^{\frac{1}{2}\eta_1}\{F_1 - z(F_2 + F_1)\} \quad \text{as } \eta_1 \to -\infty, \tag{5.30}$$

$$\frac{\partial^2 \bar{\chi}_1}{\partial \eta_1^2} \sim \frac{(1 + \frac{1}{4}\alpha_1 Br)^{\frac{1}{4}}}{8\alpha_1} e^{-\frac{1}{2}\eta_1}\{F_2 + F_1\} \quad \text{as } \eta_1 \to -\infty. \tag{5.31}$$

The inner layer problem is now specified by differential equations (5.4)–(5.5) and boundary conditions (5.12), (5.13), (5.14), (5.30) and (5.31), where $b = 1$.

The outer layer at $x \sim \ln(L_*^2 E_*)^{-1}$ or $r^2 \sim \alpha_2$ brings χ to its pure diffusive value at the rotation axis. The inner layer at $x \sim \ln(L_* E_*)^{-1}$ or $r^2 \sim \alpha_1$ adjusts $(\partial^2/\partial x^2)\chi$ and ψ. Just as in the inner Stewartson layer at the wall the x-derivatives of χ and ψ are significant in the inner layer, while, as in the outer Stewartson layer at the wall, only the x-derivatives of χ are important in the outer layer. On the other hand, in both Stewartson layers the exponential density gradient is negligible. In the core the strong variation of the density is the cause of the different flow regions, one dominated by inertia (the inviscid region), one dominated by radial diffusion of χ (the region between inner and outer layer in the core) and one dominated by radial diffusion of both χ and ψ (the pure diffusive region near the rotation axis).

The thicknesses of these regions are large compared to the density scale, whereas the thicknesses of the layers which couple these regions are equal to the density scale, as follows from the equations (5.4)–(5.5) and (5.23). Since the density scale is small compared to the radius, terms of the type r^2 can be approximated by a constant local value, $r^2 \sim \alpha_1$ and $r^2 \sim \alpha_2$ in inner and outer layer respectively, provided that conditions (5.8) and (5.24) are

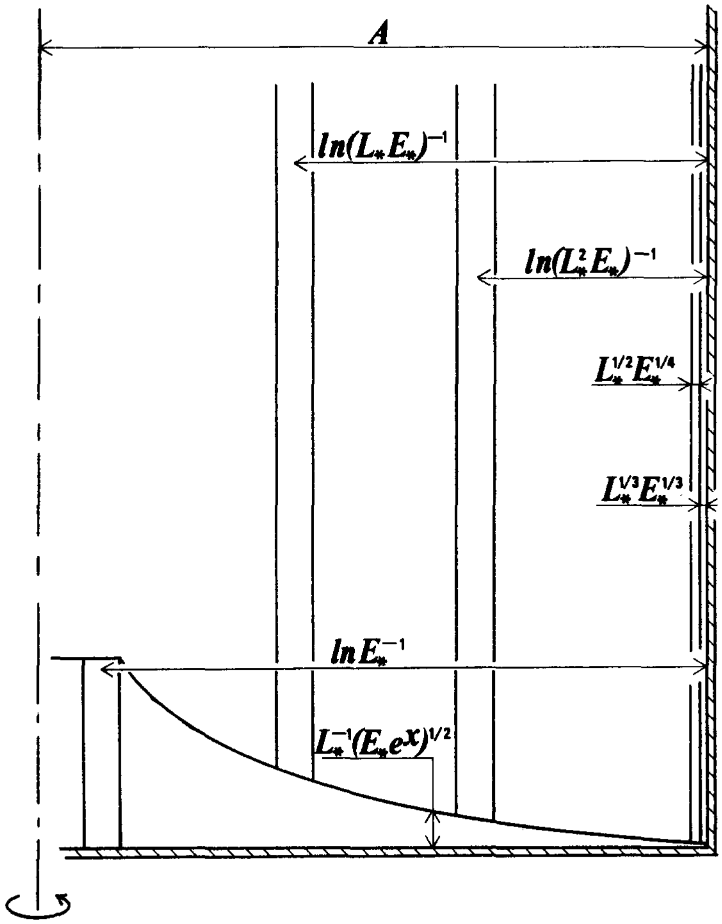

Figure 1. THE UNIT CYLINDER.

satisfied. If these conditions are not satisfied, either both layers are located in the immediate vicinity of the rotation axis $r \sim A^{-\frac{1}{2}}$ or they do not appear at all. In the latter case one observes an inviscid region up to the rotation axis. However, in gas centrifuges this is certainly not the case. Taking $L = 1$, $A = 17$ ($L_* = 17$) and $E_* = 10^{-4}$ one finds $\alpha_1 = 0.62$ and $\alpha_2 = 0.79$. Having in mind that $L \geq 1$ and that α_1 and α_2 increase with L, it is clear that if there is an inviscid region it is only observed in a small region near the cylinder wall. As already stated, the Ekman layers increase in thickness with distance from the cylinder wall and at $x \sim \ln E_*^{-1}$, where the thickness is $\sim L_*^{-1}$, also radial diffusion becomes important. For $x \gg \ln E_*^{-1}$ and $z \sim L_*^{-1}$ all diffusive terms remain comparable with each other but dominate over the inertia terms.

The inner and outer layer in the core are situated at a radial position that falls within the range $x \ll \ln E_*^{-1}$. Therefore, the complicated "all terms regions" do not need to be considered in order to describe the flow in both layers in the core. Figure 1 illustrates the various flow regions in THE UNIT CYLINDER.

The flow in the core of the cylinder has been analysed using a Navier–Stokes model. Due to the low density with correspondingly long mean free paths, this may become invalid near the rotation axis. The mean free path is comparable to the density scale when $x \sim \ln(E_*/A^{\frac{1}{2}})^{-1}$, which falls within the pure diffusive region since $A \gg 1$ and $L_* \gg 1$. Hence, the matching of the various layers occurs farther out toward the cylinder wall and remains unaffected.

6. The semi-long and long cylinder

The description in terms of an inviscid flow extended by Stewartson layers at the wall and viscous layers in the core is valid if $1 \ll L_* \ll E_*^{-\frac{1}{2}}$. Since L_* can reach considerable magnitudes, the fluid motion where L_* exceeds the upper limit of this range is also of interest. For this purpose we consider the distance scales of both layers in the core and the thickness scales of both Stewartson layers. For $L_* \sim E_*^{-\frac{1}{2}}$ the outer Stewartson layer expands over the density scale. Simultaneously the outer layer in the core comes up and joins the Stewartson layer. For $L_* \sim E_*^{-1}$ the inner Stewartson layer and the inner layer in the core expand and come up, respectively, and join. One expects that for $E_*^{-\frac{1}{2}} \sim L_* \ll E_*^{-1}$, referred to as THE SEMI-LONG CYLINDER, the x-derivatives of χ in (5.2) become important in the entire cylinder. For $L_* \sim E_*^{-1}$, referred to as THE LONG CYLINDER, the x-derivatives of ψ in (5.1) will do the same. The Ekman layer retains its small thickness and is still the region within which the flow is adjusted to the end caps.

At first the flow in THE SEMI-LONG CYLINDER is discussed. The x-derivatives of χ become important by putting

$$\chi = L_*^{-1} E_*^{-\frac{1}{2}} \chi_1, \quad \psi = E_*^{\frac{1}{2}} \psi_1. \tag{6.1}$$

Here, the magnitude of ψ corresponds to the induced flux of the Ekman layers. Substituting (6.1) into (5.1)–(5.2) and letting $L_*^2 E_*^2 \to 0$ we get

$$\frac{\partial \chi_1}{\partial z} = 0, \tag{6.2}$$

$$-\frac{\partial \psi_1}{\partial z} = 2e^x \left(1 - \frac{x}{A}\right)^{-1} \frac{\partial}{\partial x} \left\{1 + \tfrac{1}{4} Br \left(1 - \frac{x}{A}\right)\right\}^{-1} \left(1 - \frac{x}{A}\right)^2 \frac{\partial \chi_1}{\partial x}. \tag{6.3}$$

Applying the Ekman suction conditions one finds from (6.2) and (6.3) that

$$\psi_1 = \frac{1}{2}\left\{1 + \tfrac{1}{4} Br \left(1 - \frac{x}{A}\right)\right\}^{-\frac{3}{4}} \times$$
$$\times\, e^{\frac{1}{2}x} \{\tfrac{1}{2}F_1 + L_*^{-1} E_*^{-\frac{1}{2}} \chi_1 - z(\tfrac{1}{2}F_1 + \tfrac{1}{2}F_2 + 2L_*^{-1} E_*^{-\frac{1}{2}} \chi_1)\}. \tag{6.4}$$

Putting (6.4) into (6.3) one gets

$$2\left\{1 + \tfrac{1}{4} Br \left(1 - \frac{x}{A}\right)\right\}^{\frac{3}{4}} e^{\frac{1}{2}x} \left(1 - \frac{x}{A}\right)^{-1} \frac{d}{dx}\left\{1 + \tfrac{1}{4} Br \left(1 - \frac{x}{A}\right)\right\}^{-1} \times$$
$$\times \left(1 - \frac{x}{A}\right)^2 \frac{d\chi_1}{dx} - L_*^{-1} E_*^{-\frac{1}{2}} \chi_1 = \tfrac{1}{4}(F_1 + F_2). \tag{6.5}$$

Equations (6.4) and (6.5) describe the flow in the region between the inner layer in the core and the inner Stewartson layer at the cylinder wall: $0 < x \ll \ln(L_* E_*)^{-1}$. In the region $x \sim 1$ the term $1 - x/A$ can be approximated by 1 by which (6.5) simplifies to

$$2(1 + \tfrac{1}{4}Br)^{-\frac{1}{4}} e^{\frac{1}{2}x} \frac{d^2\chi_1}{dx^2} - L_*^{-1} E_*^{-\frac{1}{2}} \chi_1 = \tfrac{1}{4}(F_1 + F_2). \tag{6.6}$$

For $x \to \infty$ χ_1 must match the inner layer in the core and for $x \to 0$ χ_1 must match the inner Stewartson layer at the cylinder wall. In the inner Stewartson layer and in the inner layer in the core, however, χ is continuous up to $O(L_*^{-\frac{1}{3}} E_*^{\frac{1}{6}})$ and up to $O(L_*^{-\frac{1}{2}})$, respectively. Therefore χ_1 is directly brought to zero and to its pure diffusive value, respectively: i.e.

$$\chi_1 = 0 \qquad \text{at } x = 0, \tag{6.7}$$

$$(\partial/\partial x)\chi_1 \sim 0 \qquad \text{as } x \to \infty. \tag{6.8}$$

The differential equation (6.6) with boundary conditions (6.7) and (6.8) can be solved by applying Greens' functions with the modified Bessel functions of zero order as kernel [12].

In the region $0 \ll x \ll \ln(L_* E_*)^{-1}$ the first term on the left of (6.5) dominates over the second one (since $e^{\frac{1}{2}x}$ is large) with the result that

$$\frac{d}{dx}\left\{1 + \tfrac{1}{4}Br\left(1 - \frac{x}{A}\right)\right\}^{-1}\left(1 - \frac{x}{A}\right)^2 \frac{d\chi_1}{dx} = \\ = \frac{1}{8}\left\{1 + \tfrac{1}{4}Br\left(1 - \frac{x}{A}\right)\right\}^{-\frac{3}{4}}\left(1 - \frac{x}{A}\right) e^{-\frac{1}{2}x}(F_1 + F_2). \tag{6.9}$$

According to (6.9) $\chi_1 \sim \mathrm{e}^{-\frac{1}{2}x} F_1, e^{-\frac{1}{2}x} F_2$ and since $x \gg 0$ (6.4) may be simplified to

$$\psi_1 = \frac{1}{4}\left\{1 + \tfrac{1}{4}Br\left(1 - \frac{x}{A}\right)\right\}^{-\frac{3}{4}} e^{\frac{1}{2}x}\{F_1 - z(F_1 + F_2)\}. \tag{6.10}$$

Solution (6.4) does not allow the boundary condition for ψ at $x = 0$ to be satisfied. Therefore the inner Stewartson layer is needed. The inner layer in the core adjusts ψ to its pure diffusive value near the rotation axis. The equations and boundary conditions are the same as those given in connection with THE UNIT CYLINDER. A diagram of the various flow regions in THE SEMI-LONG CYLINDER is given in figure 2.

In the particular case that the imposed boundary conditions are antisymmetric with respect to the mid-plane $z = \frac{1}{2}$, $F_1 = -F_2$, the solution from (6.4) and (6.5) is identical with the inviscid one. This situation, of course, could be expected since for $F_1 = -F_2$ χ is zero in the inviscid region. Then no outer Stewartson layer and no outer layer in the core are needed and expansion of these layers is irrelevant. The flows in THE UNIT CYLINDER and THE SEMI-LONG CYLINDER are the same.

Finally the flow in THE LONG CYLINDER is discussed. Introducing

$$\chi = E_*^{\frac{1}{2}} \chi_2, \; \psi = E_*^{\frac{1}{2}} \psi_2, \tag{6.11}$$

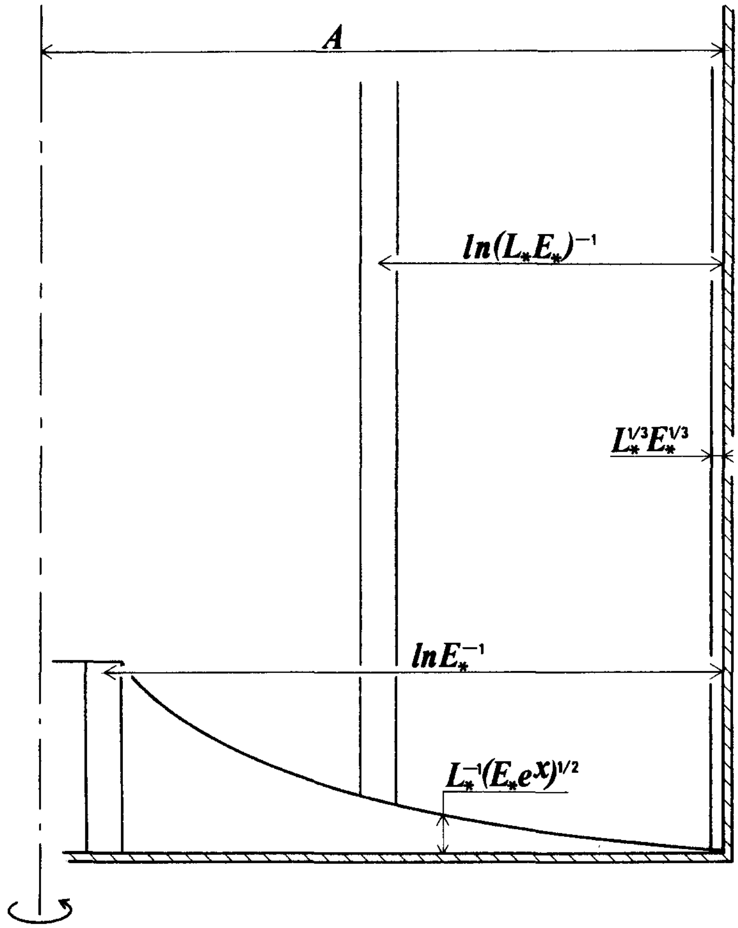

Figure 2. THE SEMI-LONG CYLINDER.

and approximating $1 - x/A$ by 1, equations (5.1) and (5.2) become

$$\frac{\partial \chi_2}{\partial z} = 8L_*E_*\left\{\frac{\partial}{\partial x}e^x\frac{\partial}{\partial x}\right\}^2 e^{-x}\psi_2, \tag{6.12}$$

$$-(1+\tfrac{1}{4}Br)\frac{\partial \psi_2}{\partial z} = 2L_*E_*e^x\frac{\partial^2 \chi_2}{\partial x^2}. \tag{6.13}$$

Eliminating χ_2 from (6.12) and (6.13) it follows that

$$16L_*^2E_*^2e^x\frac{\partial^2}{\partial x^2}\left\{\frac{\partial}{\partial x}e^x\frac{\partial}{\partial x}\right\}^2 e^{-x}\psi_2 + (1+\tfrac{1}{4}Br)\frac{\partial^2 \psi_2}{\partial z^2} = 0, \tag{6.14}$$

the solution of which is given by

$$\psi_2 = \sum_{k=1}^{\infty}\left[a_k \exp\left\{-\frac{\sqrt{\lambda_k}L_*E_*z}{(1+\frac{1}{4}Br)^{\frac{1}{2}}}\right\} + b_k \exp\left\{+\frac{\sqrt{\lambda_k}L_*E_*z}{(1+\frac{1}{4}Br)^{\frac{1}{2}}}\right\}\right]f_k(x), \tag{6.15}$$

where f_k satisfies the differential equation

$$16e^x \frac{d^2}{dx^2}\left\{\frac{d}{dx}e^x\frac{d}{dx}\right\}^2 e^{-x}f_k + \lambda_k f_k = 0. \tag{6.16}$$

The boundary conditions for f_k at $x = 0$ are deduced from (4.5a): i.e.

$$f_k = \frac{df_k}{dx} = \left\{\frac{d}{dx}e^x\frac{d}{dx}\right\}^2 e^{-x}f_k = 0 \quad \text{at } x = 0. \tag{6.17}$$

For $x \to \infty$ χ_2 and ψ_2 must match their pure diffusive values. In terms of f_4 this means

$$\frac{df_k}{dx} = \frac{d}{dx}\left\{\frac{d}{dx}e^x\frac{d}{dx}\right\}^2 e^{-x}f_k \sim 0 \quad \text{as } x \to \infty. \tag{6.18}$$

The basic solutions of the non-self-adjoint differential equation (6.16) are

$$f_k = \beta_{10} + \beta_{11}e^{-2x} + \beta_{12}e^{-4x} + \ldots, \tag{6.19a}$$

$$\beta_{20}e^{-x} + \beta_{21}e^{-3x} + \beta_{22}e^{-5x} + \ldots, \tag{6.19b}$$

$$\beta_{30}xe^{-x} + \beta_{31}xe^{-3x} + \beta_{32}xe^{-5x} + \ldots, \tag{6.19c}$$

$$\beta_{40}x + \beta_{41}xe^{-2x} + \beta_{42}xe^{-4x} + \ldots, \tag{6.19d}$$

$$\beta_{50}x^2e^{-x} + \beta_{51}x^2e^{-3x} + \beta_{52}x^2e^{-5x} + \ldots, \tag{6.19e}$$

$$\beta_{60}e^{x} + \beta_{61}x^3e^{-x} + \beta_{62}x^3e^{-3x} + \beta_{63}x^3e^{-5x} + \ldots, \tag{6.19f}$$

where β_{1i}, β_{2i}, β_{3i}, β_{4i}, β_{5i} and β_{6i}, $i \geq 1$, are a linear function of the basic coefficients β_{10}, β_{20}, β_{30}, β_{40}, β_{50} and β_{60}. In order to satisfy the boundary conditions (6.18) β_{40}, β_{50} and β_{60} must be set equal to zero. As a result, the solutions (6.19d), (6.19e) and (6.19f) can be dropped, whence

$$f_k = \sum_{i=0}^{\infty} \beta_{1i}e^{-2ix} + e^{-x}\sum_{i=0}^{\infty} \beta_{2i}e^{-2ix} + xe^{-x}\sum_{i=0}^{\infty} \beta_{3i}e^{-2ix}. \tag{6.20}$$

Application of two of the three boundary conditions (6.17) expresses β_{20} and β_{30} in β_{10}. Then, β_{1i}/β_{10}, β_{2i}/β_{10} and β_{3i}/β_{10}, $i \geq 0$, are a function of λ_k only. The remaining condition at $x = 0$ is satisfied for an infinite series of positive real eigenvalues of λ_k, $k = 1, 2, \ldots, \infty$, where the eigenvalues are ordered such that $\lambda_k < \lambda_{k+1}$. The two lowest eigenvalues are $\sqrt{\lambda_1} = 9.64$ and $\sqrt{\lambda_2} = 60.4$.* A good approximation for the first eigenfunction is given by $f_1 = 1 - 0.60e^{-x} - 0.48e^{-2x} + 0.08e^{-3x} - 1.35xe^{-x} + 0.03xe^{-3x}$ [12]. Substituting (6.11) into (4.13) and letting $E_*^{\frac{1}{2}} \to 0$, the Ekman suction conditions become

$$\psi_2 = +\tfrac{1}{4}(1 + \tfrac{1}{4}Br)^{-\frac{1}{4}}e^{\frac{1}{4}x}F_1 \qquad \text{at } z = 0, \tag{6.21}$$

* The solutions corresponding to $\lambda_k = 0$ are incompatible with the boundary conditions (6.17) and (6.18).

$$\psi_2 = -\tfrac{1}{4}(1 + \tfrac{1}{4}Br)^{-\frac{3}{4}} e^{\frac{1}{2}x} F_2 \quad \text{at } z = 1, \tag{6.22}$$

where, as before, $1 - x/A$ is approximated by 1. These boundary conditions can be used to determine the constants a_k and b_k in solution (6.15). Therefore we must expand $e^{\frac{1}{2}x}F_1$ and $e^{\frac{1}{2}x}F_2$ into the eigenfunctions f_k applying the orthogonality relation

$$\int_0^\infty f_k g_j e^{-x} dx = 0 \quad \text{for } k \neq j, \tag{6.23}$$

where g_j is the adjoint eigenfunction defined by

$$g_j = \left\{ \frac{d}{dx} e^x \frac{d}{dx} \right\}^2 e^{-x} f_j. \tag{6.24}$$

The solution for χ_2 is

$$\chi_2 = -8(1 + \tfrac{1}{4}Br)^{\frac{1}{4}} \sum_{k=1}^{\infty} \lambda_k^{-\frac{1}{2}} \left[a_k \exp\left\{ -\frac{\sqrt{\lambda_k} L_* E_* z}{(1 + \frac{1}{4}Br)^{\frac{1}{2}}} \right\} \right.$$
$$\left. - b_k \exp\left\{ + \frac{\sqrt{\lambda_k} L_* E_* z}{(1 + \frac{1}{4}Br)^{\frac{1}{2}}} \right\} \right] g_k(x). \tag{6.25}$$

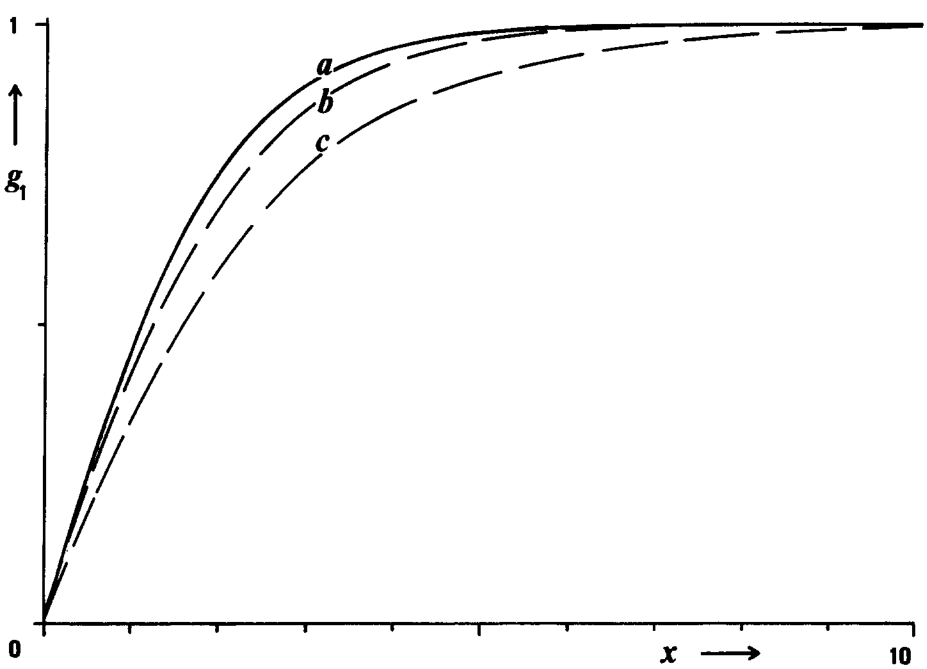

Figure 3. First eigenfunction of χ versus x.
a: Asymptotic solution
b: Parker & Mayo's solution for $A = 16$
c: Parker & Mayo's solution for $A = 9$.

A differential equation similar to (6.14) has recently been studied by Bark & Bark [14] and Durivault & Louvet [15]. However, these authors arrived at this equation by considering the inner Stewartson layer with a varying density. In these studies the boundary conditions are anti-symmetric with respect to $z = \frac{1}{2}$ ($F_1 = -F_2$ in the present work) and $x = (L_* E_*)^{\frac{1}{2}} \zeta$, where ζ is the boundary layer coordinate and $(L_* E_*)^{\frac{1}{2}}$ is the ratio of the boundary layer thickness to the density scale. In contrast with the suggestions of these authors, the above presented solutions show that for $L_* E_* \approx 1$ the flow behaves in a diffusive manner over the entire cross-section of the cylinder. This finds expression in the decaying behaviour with respect to z, with the result that at a reasonable distance from both end caps the flow is mostly described by the first eigenfunction. In fact, it is impossible to find solutions from (6.14) which satisfy the boundary conditions (6.17), (6.21) and (6.22), and which match an inviscid flow as $x \to \infty$!

In case of a cylinder of semi-infinite length b_k must be set equal to zero in (6.15) and (6.25). This is the situation considered by Ging [8], similar to the one of Dirac [6], but including effects due to heat conduction ($Br \neq 0$ in (6.15) and (6.25)). Steenbeck [7] and Parker & Mayo [9] treated the semi-infinite cylinder without applying an asymptotic solution for large A but calculated numerically the radial shape of the first eigenfunction for various magnitudes of A. In figure 3 we have compared Parker & Mayo's calculation of g_1 for $A = 9$ and $A = 16$ to the asymptotic solution, where we took $g_1 = 1$ as $x \to \infty$. One sees that the agreement is already good for $A = 16$. The same conclusion applies to the radial shape of f_1 and the first eigenvalue.

Acknowledgements

The author wishes to thank Professor L. van Wijngaarden for his critical discussion and careful reading of this paper. Thanks are also due to Professor J. Los for his continuous interest in this work. Mr. C. A. Andrews is acknowledged for his comments on the English text.

REFERENCES

[1] H. Mikami, Thermally induced flow in gas centrifuge (1), *J. Nucl. Sci. Technol.* 10 (1973) 396–401.
[2] H. Mikami, Thermally induced flow in gas centrifuge (2), *J. Nucl. Sci. Technol.* 10 (1973) 580–583.
[3] W. Nakayama and S. Usui, Flow in rotating cylinder of a gas centrifuge, *J. Nucl. Sci. Technol.* 11 (1974) 242–262.
[4] T. Sakurai and T. Matsuda, Gasdynamics of a centrifugal machine, *J. Fluid Mech.* 62 (1974) 727–736.
[5] H. P. Greenspan, *The theory of rotating fluids*, Camb. Univ. Press (1968).
[6] P. A. M. Dirac, *The motion in a self-fractioning centrifuge*, General Electric, Schenectady, New York, Rep. Br-42 (1940).
[7] M. Steenbeck, Erzeugung einer Selbstkaskadierenden Axialströmung in einer langen Ultrazentrifuge zur Isotopentrennung, *Kernenergie* 1 (1958) 921–928.
[8] J. L. Ging, *Countercurrent flow in a semi-infinite gas centrifuge: axially symmetric solution in the limit of high angular speed*, Univ. of Virginia, Charlottesville, Rep. EP-4422-198-62S (1962).
[9] H. M. Parker and T. T. Mayo, *Countercurrent flow in a semi-infinite gas centrifuge – preliminary results*, Univ. of Virginia, Charlottesville, Rep. EP-4422-279-63U (1963).
[10] R. B. Bird, W. E. Stewart and E. N. Lightfoot, *Transport phenomena*, John Wiley & Sons, New York (1960).

[11] K. Stewartson, On almost rigid rotations, *J. Fluid Mech.* 3 (1957) 17–26.

[12] J. J. H. Brouwers, *On the motion of a compressible fluid in a rotating cylinder*, Ph.D. Thesis, Thesis, Twente Univ. of Technology, Enschede, The Netherlands (1976).

[13] K. Stewartson, On almost rigid rotations. Part 2, *J. Fluid Mech.* 26 (1966) 131–144.

[14] F. H. Bark and T. H. Bark, On vertical boundary layers in a rapidly rotating gas, *J. Fluid Mech.* 78 (1976) 749–761.

[15] J. Durivault and P. Louvet, Etude de la couche de Stewartson compressible dans une centrifugeuse à contre-courant thermique, *C. R. Acad. Sc. Paris* t. 283 série B (1976) 79–82.